PNAS
www.pnas.org

Supplementary Information for
Structures and implications of TBP-nucleosome complexes

Haibo Wang[a], Le Xiong[a] Patrick Cramer[a,*]

[a]Max Planck Institute for Biophysical Chemistry, Department of Molecular Biology, Am Fassberg 11, 37077 Göttingen, Germany.

*Corresponding author.

Email: patrick.cramer@mpibpc.mpg.de

This PDF file includes:

Other supplementary materials for this manuscript include the following:

Movie S1

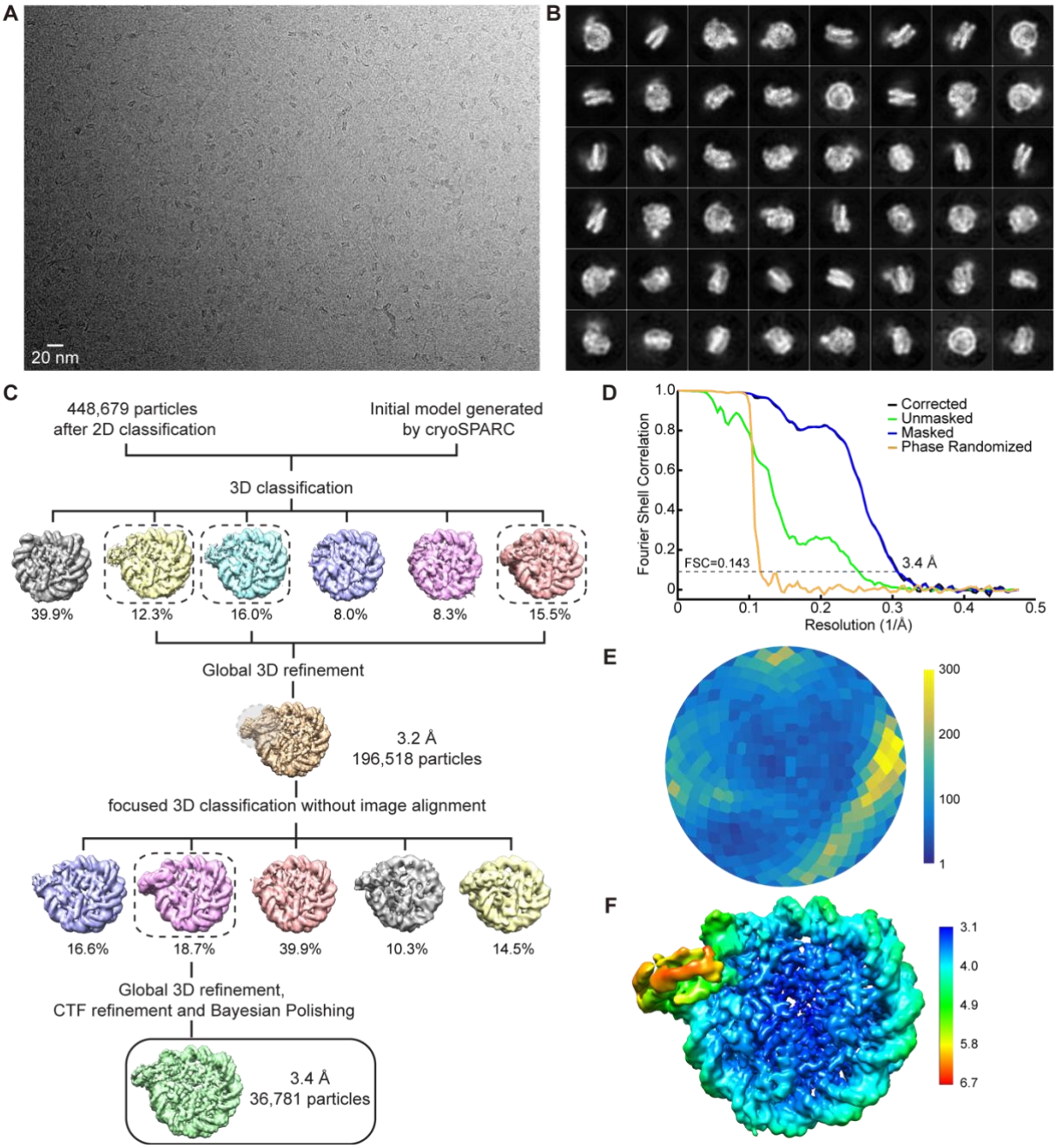

Fig. S1. Cryo-EM structure determination of TBP-NCP complex. (*A*) Exemplary cryo-EM micrograph. (*B*) Representative 2D class averages. (*C*) Sorting and classification tree. (*D*) Fourier shell correlation (FSC) between half maps of the final reconstructions. Resolutions for the gold-standard FSC 0.143 criterion are listed. (*E*) Angular distribution plot for particles in the final reconstruction. Color shading from blue to yellow provides the number of particles at a specific orientation as indicated. (*F*) Surface representation of the structure colored according to local resolution (Å).

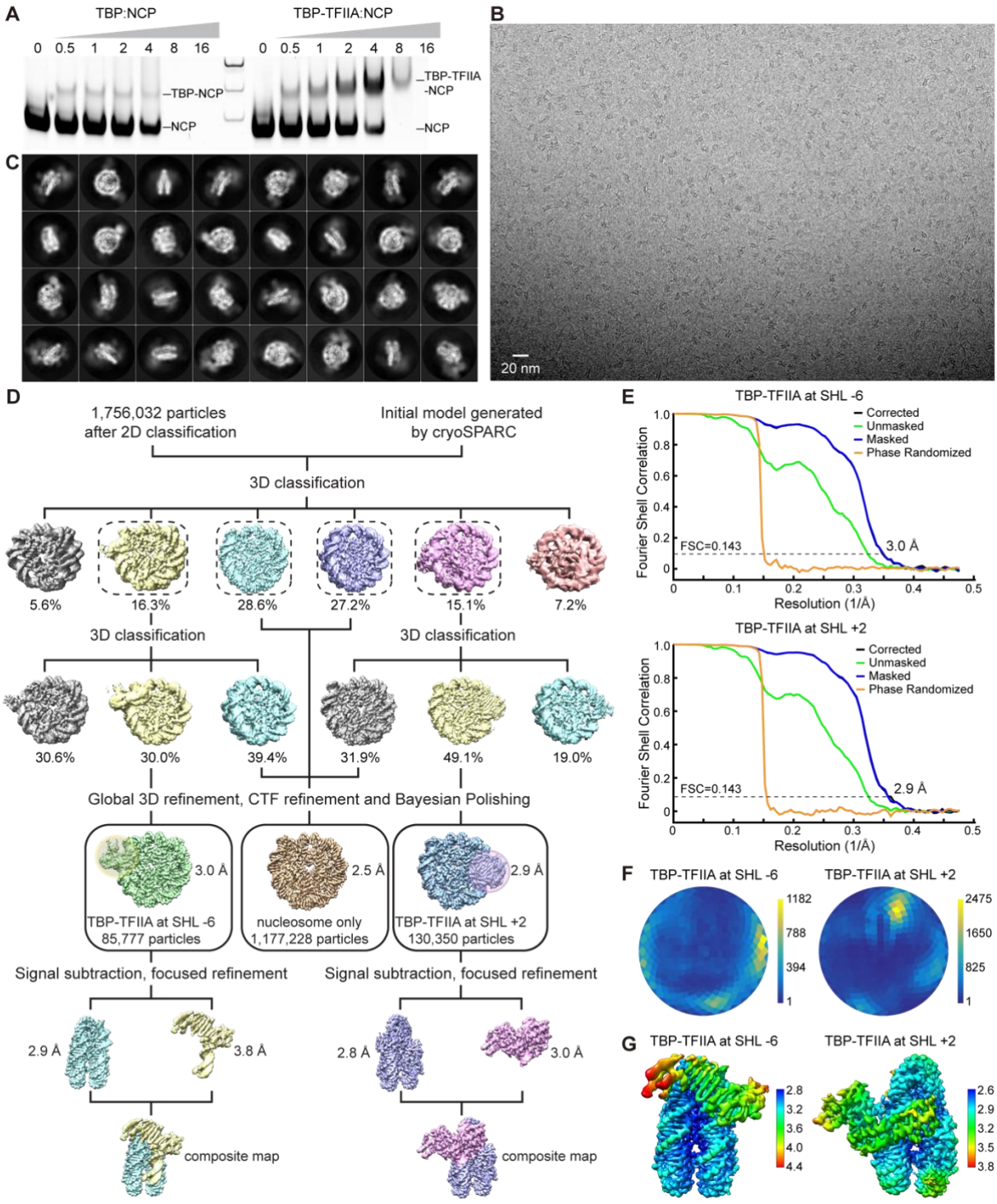

Fig. S2. Sample preparation and cryo-EM structure determination of TBP-TFIIA-NCP complex. (*A*) Electrophoretic mobility shift assay (EMSA) shows that TFIIA stabilizes TBP binding to the nucleosome. Molar ratios of TBP to NCP or TBP/TFIIA to NCP are shown on the top of each lane. Bands are labeled on the right. (*B*) Exemplary cryo-EM micrograph. (*C*) Representative 2D class averages. (*D*) Sorting and classification tree. (*E*) Fourier shell correlation (FSC) between half maps of the final reconstruction. Resolutions for the gold-standard FSC 0.143 criterion are listed. (*F*) Angular distribution plot for all particles in the final reconstruction. Color shading from blue to yellow provides the number of particles at a specific orientation. (*G*) Surface representation colored according to local resolution (Å).

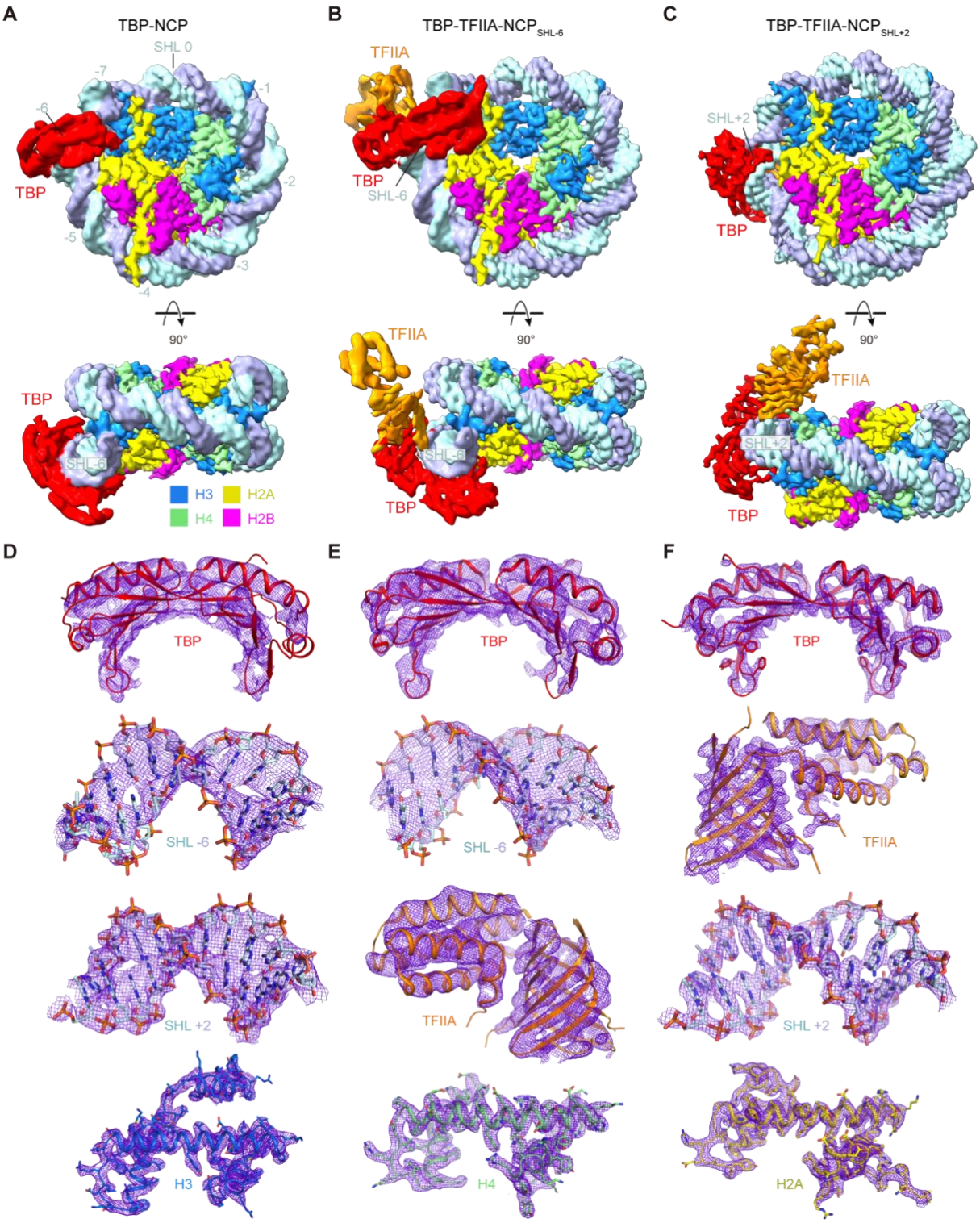

Fig. S3. Quality of the cryo-EM densities. (*A-C*) Overall cryo-EM maps of the structures TBP-NCP, TBP-TFIIA-NCP$_{SHL-6}$ and TBP-TFIIA- NCP$_{SHL+2}$, respectively. (*D-F*) Local map densities (purple meshes) for various regions as indicated for TBP-NCP (*D*), TBP-TFIIA-NCP$_{SHL-6}$ (*E*), and TBP-TFIIA- NCP$_{SHL+2}$ (*F*).

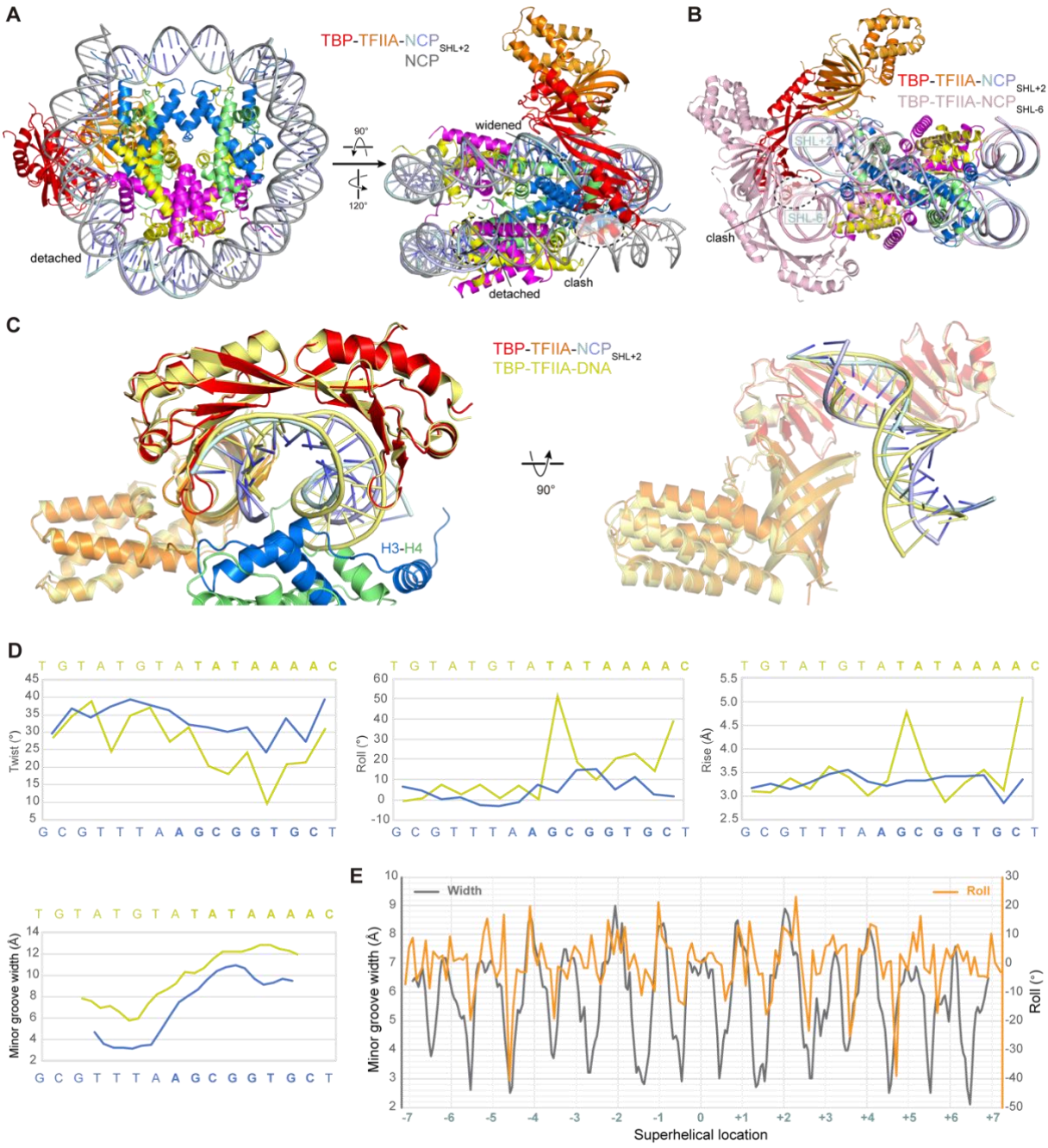

Fig. S4. DNA conformation in TBP-TFIIA-NCP$_{SHL+2}$ structure. (*A*) Comparison with unbound NCP structure after superposition of histones. (*B*) Comparison with TBP-TFIIA-NCP$_{SHL-6}$ structure are superposition of histones. (*C*) Comparison with TBP-TFIIA-DNA structure (PDB code: 1YTF) (1) after superposition of TBP proteins shows the difference of underlying DNA in inclinations of base pairs. (*D*) Comparison of the DNA base-pair-step parameters and minor groove width in TBP-TFIIA-NCP$_{SHL+2}$ (blue) and TBP-TFIIA-DNA (yellow). The base-pair-step parameters twist, roll and rise, and the minor groove width of DNA were calculated using CURVES+ (2). DNA nucleotides covered by TBP are in boldface. (*E*) Plot of minor groove widths (grey) and roll angles (orange) in the unbound Widom 601 NCP structure.

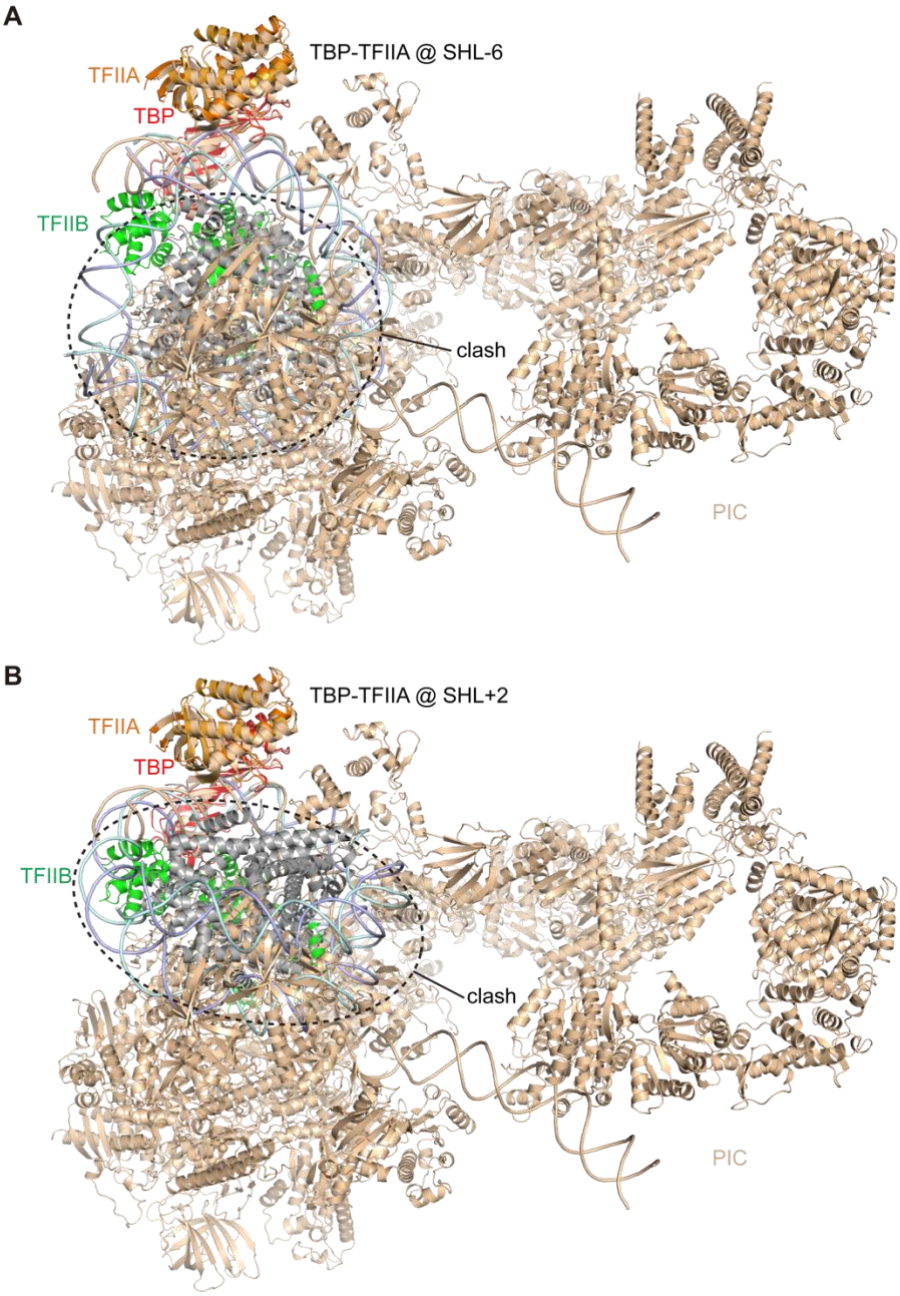

Fig. S5. Nucleosome-bound TBP is incompatible with PIC assembly. (*A*) Comparison of the TBP-TFIIA-NCP_{SHL-6} structure with the PIC structure (PDB code: 5OQJ) (3) after superposition of TBP. (*B*) Comparison of the TBP-TFIIA-NCP_{SHL+2} structure with the PIC structure after superposition of TBP. Histones are in grey whereas PIC components are in wheat except for TFIIB, which is in green.

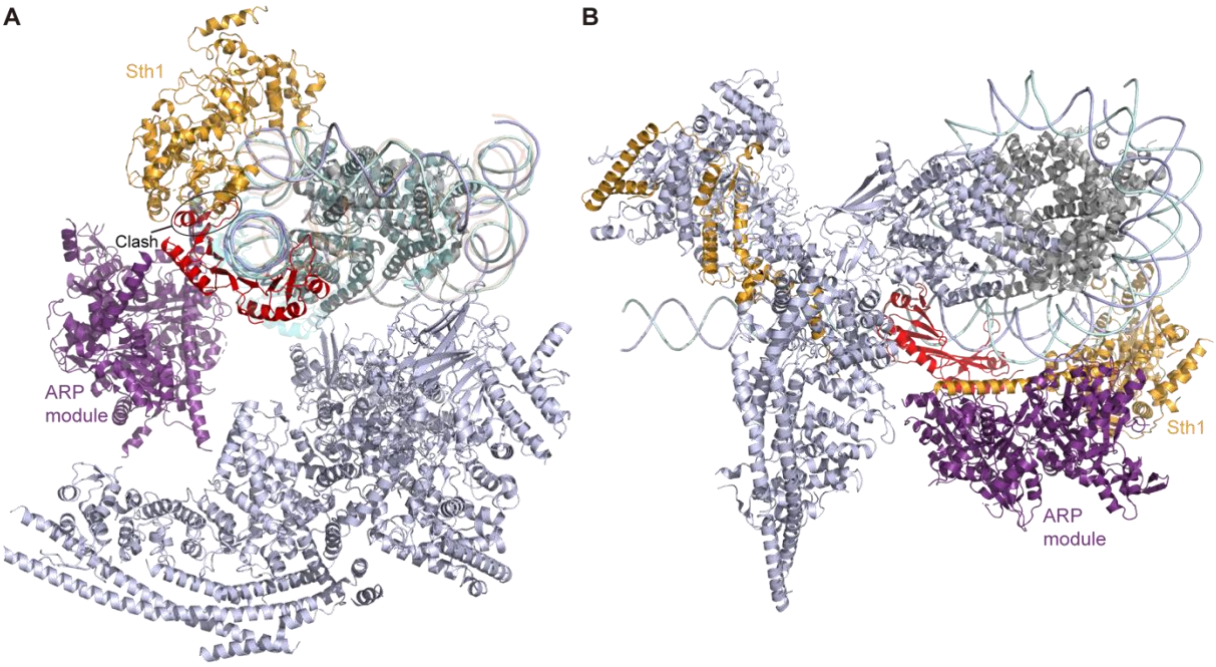

Fig. S6. TBP may be accommodated during chromatin remodeling by RSC. (A) Modeling TBP (red) at SHL –6 of a RSC-nucleosome structure (PDB 6KW3) (4) clashes with ATPase motor module (gold), as indicated with a black circle. (B) Modeling TBP (red) at SHL –7 of a RSC-nucleosome structure containing longer upstream DNA (PDB 6TDA) (5) does not result in clashes between TBP and RSC.

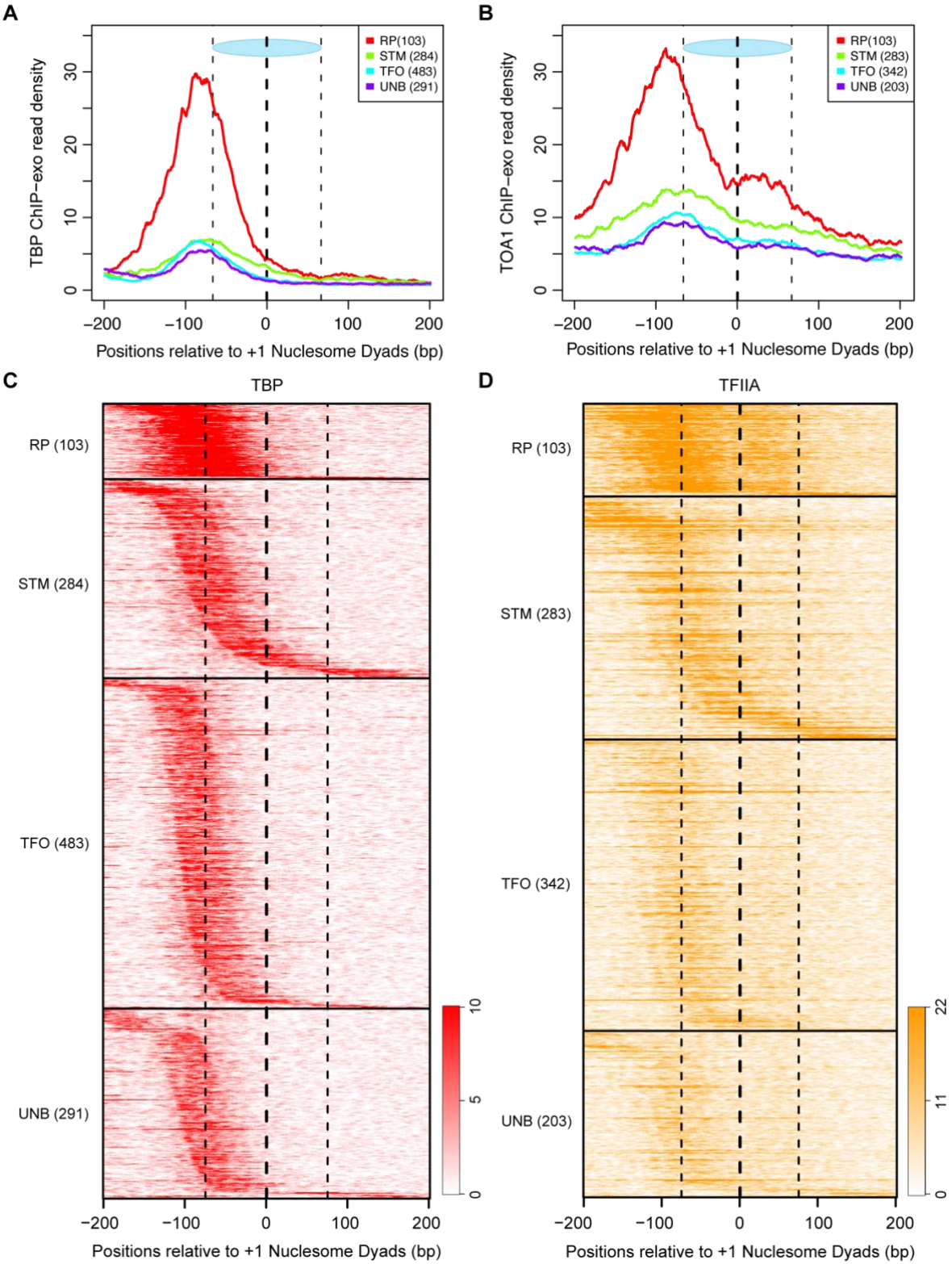

Fig. S7. Distribution of TBP and TFIIA ChIP-exo genome-wide occupancy (6) with respect to the location of the +1 nucleosome in yeast cells. The blue oval denotes the nucleosome with its boundaries shown as vertical dashed lines. (*A-B*) Metagene plots of TBP (panel *A*) and TFIIA (panel *B*) occupancy around the +1 nucleosome for four subgroups of genes (6) as follows: RP: genes encoding ribosomal proteins; STM: genes with promoters associated with inducibility, characteristically bound by sequence-specific transcription factors and major cofactor meta-assemblages SAGA, TUP and/or Mediator/SWI–SNF; TFO: genes with promoters that lacked STM cofactors but typically contained the insulator Abf1 or Reb1; UNB: genes with promoters that only showed bound PIC. (*C-D*) Heatmaps of TBP and TFIIA occupancy

around the +1 nucleosome sorted by the distance between the two for four subgroups of genes as in panels *A*, *B*.

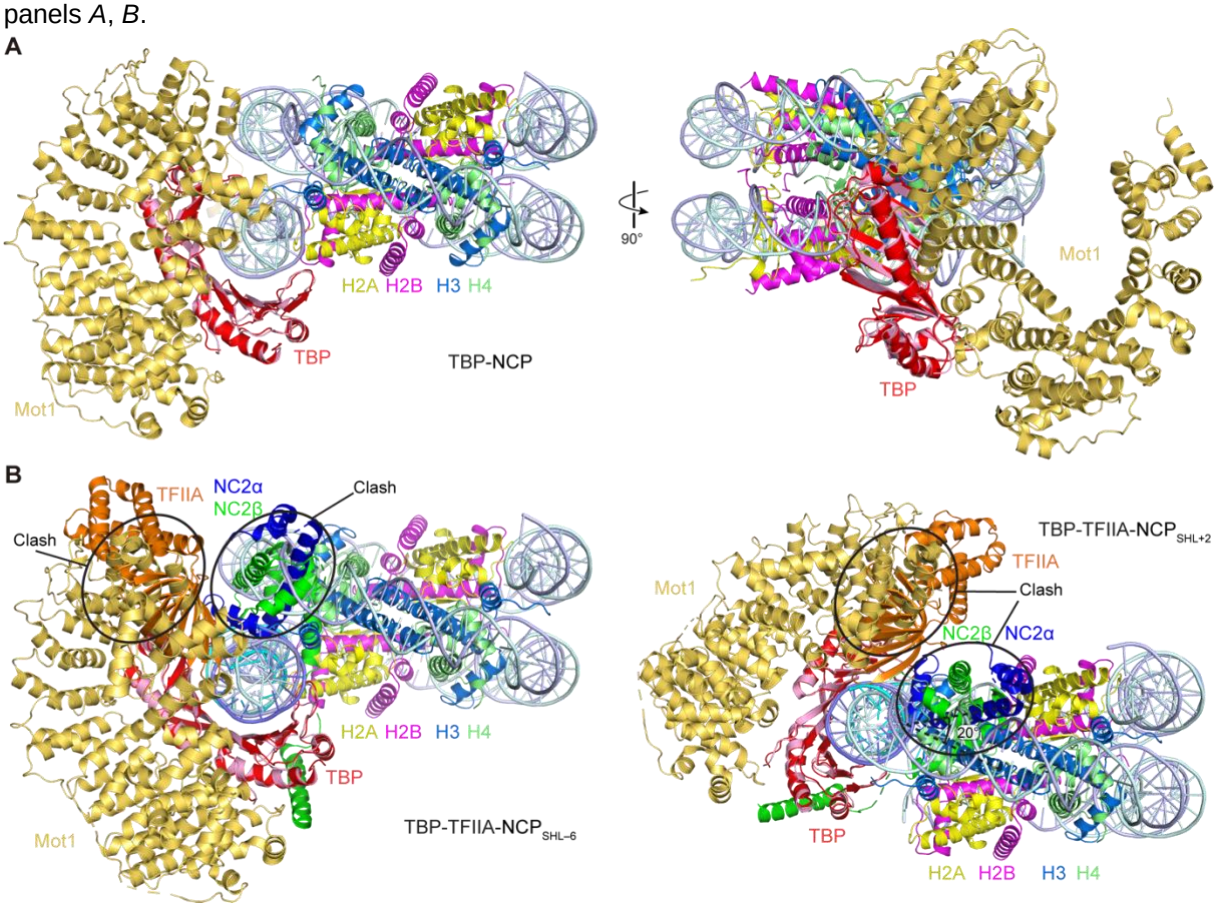

Fig. S8. Comparisons with structures of the TBP regulators Mot1 and NC2. (*A*) Comparison of our TBP-NCP structure with the Mot1-TBP complex structure (PDB 3OC3) (7) after superposition of TBP suggests that N-terminal domain of Mot1 can bind nucleosome-bound TBP. The latch motif of Mot1 is omitted. (*B*) Comparison of our two TBP-TFIIA-NCP structures with the Mot1-TBP-DNA-NC2 structure (PDB 4WZS) (8) after superposition of TBP. NC2 occupies a position similar to that of the histone dimer H3-H4 in the nucleosome. Clashes are indicated with black circles. Only the N-terminus of Mot1 is present in the structural comparisons.

Supplementary references

1. S. Tan, Y. Hunziker, D. F. Sargent, T. J. Richmond, Crystal structure of a yeast TFIIA/TBP/DNA complex. *Nature* **381**, 127-151 (1996).
2. C. Blanchet, M. Pasi, K. Zakrzewska, R. Lavery, CURVES+ web server for analyzing and visualizing the helical, backbone and groove parameters of nucleic acid structures. *Nucleic Acids Res* **39**, W68-73 (2011).
3. S. Schilbach *et al.*, Structures of transcription pre-initiation complex with TFIIH and Mediator. *Nature* **551**, 204-209 (2017).
4. Y. Ye *et al.*, Structure of the RSC complex bound to the nucleosome. *Science* **366**, 838-843 (2019).
5. F. R. Wagner *et al.*, Structure of SWI/SNF chromatin remodeller RSC bound to a nucleosome. *Nature* **579**, 448-451 (2020).
6. M. J. Rossi *et al.*, A high-resolution protein architecture of the budding yeast genome. *Nature* **592**, 309-314 (2021).
7. P. Wollmann *et al.*, Structure and mechanism of the Swi2/Snf2 remodeller Mot1 in complex with its substrate TBP. *Nature* **475**, 403-407 (2011).
8. A. Butryn *et al.*, Structural basis for recognition and remodeling of the TBP:DNA:NC2 complex by Mot1. *Elife* **4** (2015).

Table S1. Curve fitting parameters for fluorescence anisotropy assay.

Fluorescence anisotropy data found in Fig. 1-2 were fit with a single site binding model. Apparent dissociation constants ($K_{d,app}$), B_{max} (maximum anisotropy) and R^2 values with error are shown.

Protein	**Substrate**	$K_{d,app}$ **(nM)**	B_{max}	R^2
TBP	Widom-601 DNA	31.1 ± 8.5	123.6 ± 3.3	0.978
TBP	Widom-601 NCP	134.2 ± 28.7	82.9 ± 3.9	0.962
TBP+TFIIA	Widom-601 NCP	103.5 ± 6.3	113.1 ± 2.4	0.992

Table S2. Cryo-EM Data collection, refinement and validation statistics.

	TBP-NCP (EMDB-12899) (PDB 7OHB)	TBP-TFIIA-NCP_{SHL-6} (EMDB-12897) (PDB 7OH9)	TBP-TFIIA-NCP_{SHL+2} (EMDB-12898) (PDB 7OHA)	Free NCP (EMDB-12900) (PDB 7OHC)
Data collection and processing				
Microscope	FEI Titan Krios	FEI Titan Krios	FEI Titan Krios	FEI Titan Krios
Detector	Gatan K3	Gatan K3	Gatan K3	Gatan K3
Magnification	81,000	81,000	81,000	81,000
Voltage (kV)	300	300	300	300
Electron exposure (e^{-}/Å^2)	41.2	40.8	40.8	40.8
Defocus range (μm)	1.5-2.5	1.5-2.5	1.5-2.5	1.5-2.5
Pixel size (Å)	1.05	1.05	1.05	1.05
Symmetry imposed	C1	C1	C1	C1
Initial particle images (no.)	448,679	1,756,032	1,756,032	1,756,032
Final particle images (no.)	36,781	85,777	130,350	1,177,228
Map resolution (Å)	3.4	3.0	2.9	2.5
FSC threshold	0.143	0.143	0.143	0.143
Map resolution range (Å)	3.1-6.7	2.8-4.4	2.6-3.8	2.3-3.6
Refinement				
Initial model used (PDB code)	3LZ0, 1YTB	3LZ0, 1NH2	3LZ0,1NH2	3LZ0
Model resolution (Å)	3.3	2.9	2.8	2.6
FSC threshold	0.5	0.5	0.5	0.5
Map sharpening *B* factor (Å^2)	-67.51	-54.20	-49.14	-43.8
Model composition				
Non-hydrogen atoms	13424	15099	14215	12019
Protein residues	943	1144	1159	764
Nucleotide residues	290	290	244	290
B factors (Å^2)				
Protein	102.5	101.78	97.11	82.16
Nucleic acid	124.23	106.47	104.20	108.75
R.m.s. deviations				
Bond lengths (Å)	0.005	0.007	0.005	0.005
Bond angles (°)	0.854	0.836	0.911	0.856
Validation				
MolProbity score	1.34	1.40	1.26	1.23
Clashscore	4.44	5.05	4.97	4.52
Poor rotamers (%)	0.89	0	0.20	0.16
Ramachandran plot				
Favored (%)	97.41	97.31	98.59	98.13
Allowed (%)	2.59	2.69	1.41	1.87
Disallowed (%)	0	0	0	0

Movie S1. Overview of TBP-nucleosome structures. The video shows the conformation change of the DNA upon TBP binding and the movement of TBP upon TFIIA binding.